Particle Size Distribution in a Stirred Tank: Comparison of Quadrature Method of Moments CFD Predictions with Analytical Solutions

Bin Wan and Terry A. Ring
Dept. Chemical Engineering
University of Utah
Salt Lake City, UT 84112

and

Kumar M. Dhanasekharan and Jayanta Sanyal
Fluent Inc.
10 Cavendish Court
Lebanon, NH 03766

Abstract

The computational fluid dynamics environment has been enhanced with a quadrature method of moments (QMOM) population balance capability that operates in conjunction with its multiphase calculations to predict the particle size distribution within the flow field. These prediction capabilities are tested in a 3-dimensional constant stirred tank with a Rushton impeller. The tank was operated under well mixed conditions as identified by the residence time distribution. For these well mixed conditions, predictions are compared with analytical solution of ideal continuous mixed suspension, mixed product removal (CMSMPR) crystallizer. The results of these QMOM simulations are compared to steady state analytical solutions for the population balance in a well mixed stirred tank where 1) combined nucleation and growth, 2) aggregation, and 3) breakage, take place separately and 4) combined nucleation, growth and aggregation takes place. The results of these comparisons show varying levels of error for the moments of the population balance. In some cases, the error is as high as 20% but that error is not due to computational inaccuracies but to the mixing that is not ideal even in a tank with a nearly ideal residence time distribution.

Keyword: Population Balance, Computational Fluid Dynamics, Crystallization, Simulation

1. Introduction

The population balance equation (PBE) is a statement of continuity for particulate systems. Cases in which a population balance applies include crystallization, precipitation, bubble columns, gas sparging, sprays, fluidized bed polymerization, granulation, wet milling, liquid-liquid dispersions, air classifiers, hydrocyclones, particle classifiers, and aerosol flows. In the case of a continuous mixed-suspension, mixed-product removal (CMSMPR) crystallizer operating at steady

state in which aggregation, breakage and growth are occurring the PBE is given by Randolph and Larson [Randolph, A. D. (1988)] as

$$\frac{n(v)-n_{in}(v)}{\tau}+\frac{d(G(v)n(v))}{dv}=b(v)-d(v) \qquad [1]$$

with the boundary condition, $n(0)=n_o(x)$. In the above equation, n(v) is the number-based population of particles in the tank which is a function of the particle volume, v. The subscript "in" refers to the inlet population. G(v) is the particle volume dependent growth rate and b(v) is the particle volume dependent birth rate and d(v) is the particle volume dependent death rate. In the case of aggregation, the birth and death rate terms are given by Hulburt and Katz [Hulburt, H. M. (1964)]:

$$b_a(v)-d_a(v)=\int_0^{v/2}\beta(v-w,w)n(v-w)n(w)dw-n(v)\int_0^{\infty}\beta(v,w)n(w)dw \qquad [2]$$

where the aggregation rate constant, β(v,w), is a measure of the frequency of collision of particles of volume, v, with those of volume, w. In the case of breakage, the birth and death rate terms are given by Prasher [Prasher, C.L. (1987)]:

$$b_b(v)-d_b(v)=\int_v^{\infty}S(w)\rho(v,w)n(w)dw-S(v)n(v) \qquad [3]$$

where S(v) is the breakage rate constant that is a function of particle volume, v. ρ(v,w) is the daughter distribution function defined as the probability that a fragment of a particle of volume w will appear in volume v.

The moments of n(v) are useful because of their physical significance. The k^{th} volume moment is defined by

$$_vm_k=\int_0^{\infty}w^k n(w)dw. \qquad [4]$$

$_vm_o$ and $_vm_1$ represent the total number and total volume of particles in the system.

Computational Fluid Dynamics (CFD) deals with equations that represent a balance process for mass, momentum, energy and chemical species. These equations are all characterized by the following generalize partial differential equation.

$$\underbrace{c\left[\frac{\partial\rho\phi}{\partial t}\right.}_{Transient}+\underbrace{\left.\frac{\partial\rho u_i\varphi}{\partial x_i}\right]}_{Convective}=\underbrace{\frac{\partial}{\partial x_i}\Gamma^{(\varphi)}\frac{\partial\varphi}{\partial x_i}}_{Diffusive}+\underbrace{S^{(\varphi)}}_{Source} \qquad [5]$$

For the momentum balance, Φ is given by individual components of the velocity vector, Γ is given by the viscosity and there are no source terms. For the energy balance, Φ is given by temperature; Γ is given by the thermal conductivity and the source term given by the heat of reaction or other heat sources. For the mass balance, Φ is given by mass fraction; Γ is given by the molecular diffusion coefficient and the source term given the rate of chemical reaction.
The population balance equation can also be described in this same form as equation 5, when it is written in the moment form of the population balance. In this case, Φ is given by several moments of the population of particles, Γ is given by the Brownian diffusivity and the source terms are due to breakage and agglomeration. To well characterize a given particle size distribution several moments are used, typically 3 to 6. In order to solve those partial differential equations for the momentum, mass, energy and population balance, finite element or finite difference methods are used. This paper uses a special type of finite difference algorithm called the finite volume method. With the quadrature method of moments (QMOM), the population balance is written as a series of moment equations by multiplying equation 1 by v^k and integrating with respect to v from zero to infinity. These moment equations are used in place of the PBE to approximate the particle size distribution, see [Randolph, A. D. (1988)]. QMOM was first proposed by McGraw [McGraw, R. (1997)] and further developed by Marchisio, et. al. [Marchisio, D.L. (2003)]. With this implementation of QMOM PBE solver, a small number of moments, N, (typically 6) are used. Moments are approximated by a quadrature approximation that uses N/2 weights, W_i, and N/2 sizes, L_i, as follows:

$$ {}_L m_k = \sum_{i=1}^{N/2} W_i L_i^k \qquad [6] $$

Upon substitution of these weights and sizes into the N moment equations, we have a series of equations that just equals the number of unknowns, N, allowing for the solution of the system of equations that constitutes an approximation of the PBE. From the moments, the particle size distribution can be reconstituted using a moment transformation [Randolph, A. D. (1988)].

The moments used in this QMOM algorithm are length based and are different from those described by equation 4 which are volume based. There is a correspondence between length based moments and volume based moments. This correspondence is given in Table 1, where K_a is the surface area shape factor, and K_v is the volume shape factor. Noting this correspondence any length-based moment can be compared with the volume based moment predicted from an analytical solution to the population balance and equation 4.

Table 1 Correspondence between length based and volume based moments

Property	Volume Based Moment	Length Based Moment
Number of Particles	${}_v m_0$	${}_L m_0$

Surface Area of Particles	$_{V}m_{2/3}$	$Ka^{*}_{L}m_{2}$
Volume of Particles	$_{V}m_{1}$	$Kv^{*}_{L}m_{3}$

In this work, a 3-D analogue is used to simulate an experimental stirred tank CMSMPR. These simulations are compared to steady-state analytical solutions to the PBE for 1) aggregation, 2) breakage, taking place separately and 3) combined nucleation and growth and 5) combined nucleation, growth and aggregation taking place. The analytical solutions for n(v) are converted to the length based moments 0 to 5 and compared directly to the length based moments predicted by the QMOM PBE algorithm.

Before this study, a residence time distribution (RTD) validation study was performed by comparing with experimental data [Choi, B-S., et. al. (2004)]. Using operating conditions where the experimental results and the fluid flow simulations gave nearly ideal residence time distributions, population balance verification simulations are performed.

2. Simulation Setup for a 3-D Stirred Tank

A model of 1.4 L stirred tank shown in Figure 1 was constructed using a rotating mesh in the region of the impeller and a fixed mesh elsewhere. There are 4 9.5 mm baffles inside the tank, as well as, two feed tubes and one thermowell placed radially between the baffles and the impeller. The feed tube is the tube that is bent with an outlet just below the impeller. The product tube is located at the fluid interface at the top of the tank at a radial position half way to the tank wall. The impeller was 45 mm in diameter and 11.25 mm in height. See [Choi, B-S., et. al., (2004)], for other geometric details. The mesh generated to model the tank contains 626,512 elements. This grid was then used for fluid flow simulations within the tank. The k-ε turbulent model was used to predict the flow profile with flow at the inlet at the feed flow rate corresponding to several of our experimental cases using a velocity input boundary condition that corresponds to plug flow. The tank output was given a pressure outlet boundary condition. The walls of the tank, baffles and the other tank internals were assigned standard wall function boundary conditions, the top surface was assigned a symmetry boundary condition, the surface of the moving zone was coupled to the fixed zone using an interface boundary condition and the surface of the impeller, inside the moving zone, was assigned a standard wall function boundary condition. The model was allowed to run until all the dimensionless residuals reached a value of 10^{-4}. This level of convergence took ~1,100 iterations. This mesh has been shown to be grid invariant for velocity field simulations. For the conditions where the inlet flow rate is 14 mL/s and a mixing rate of 80 rpm, the resulting velocity profile is given in Figure 2. Velocity field shows that the steady state solution contains the two major circulation cells one above and one below the impeller. Path lines associated with the flow suggest that the overall flow pattern is that of a helical flow around the surface two torous one above and the other below the impeller.

This overall flow pattern is interrupted by the flow around and behind the baffles. The flow behind the baffles plays an important role in passing fluid from the top circulation cell to the bottom circulation cell as there is a minor circulation cell of cylindrical form behind each baffle in which the material can enter from the top circulation cell and exit into the bottom circulation cell or vice versa. There is also some mixing of material between the two circulation cells at the plane of the impeller as the flow moves radially out, some of the fluid is exchanged from the upper circulation cell to the lower circulation cell and vice versa.

To test the accuracy of the well mixed assumption, the residence time distribution was predicted using a unit tracer concentration, a second phase with the properties of water, in the tank that is allowed to displace a first water phase as time progresses. The convective flux of the tracer at outlet is collected from this simulation and plotted against time [Choi, B-S., et. al., (2004)], then converted to residence time distribution using:

$$E(t) = \frac{dC(t)}{dt} \qquad [7]$$

The RTD determined in is way is normalized since the feed tracer concentration was 1.0. The outlet concentration predicted by the simulation is shown in Figure 3 for the turbulent flow simulations as well as the ideal curve. Here we see that the turbulent simulation is nearly identical to the ideal curve except at the start where the ideal curve instantly jumps to 1.0 at time zero and the simulation E(t) curve more slowly increases as is the case with experimental results[Choi, B-S., et. al., (2004)]. Only the turbulent flow simulation accurately predicted the ideal residence time distribution.

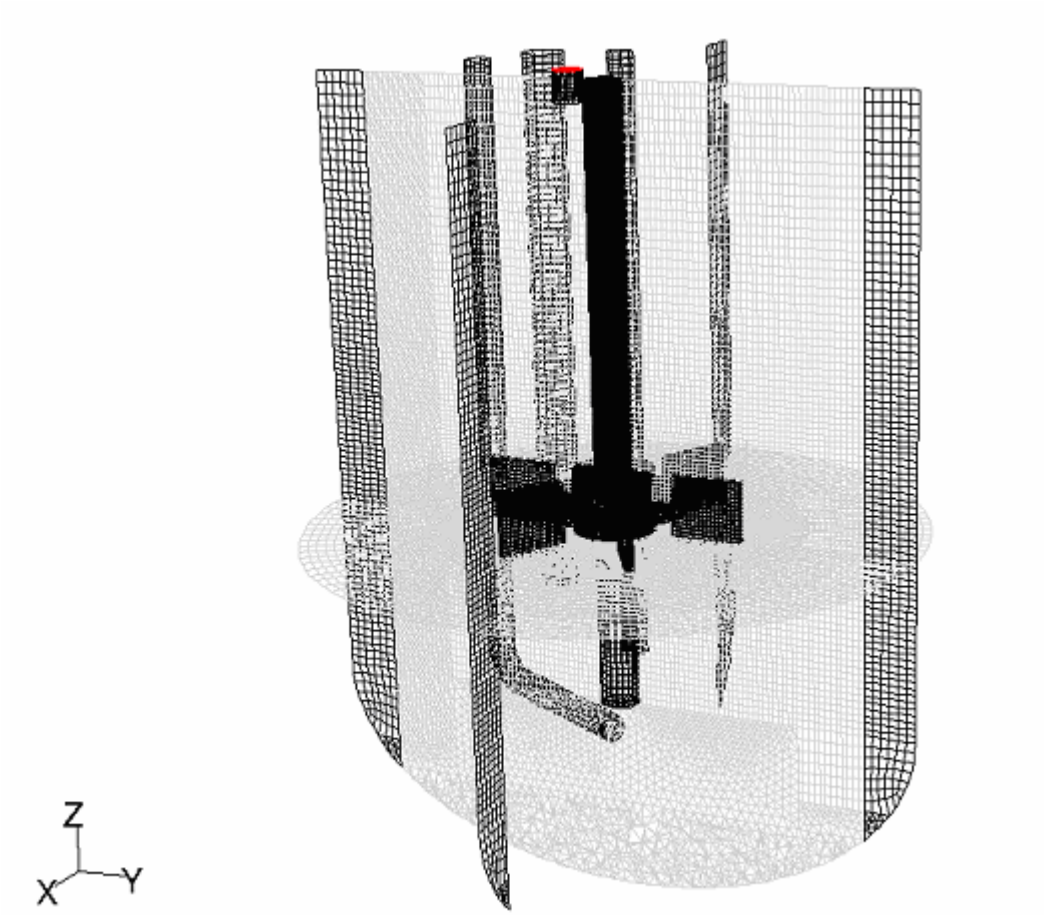

Figure 1 Geometry of 3-D stirred tank with a volume of 1.4 liter.

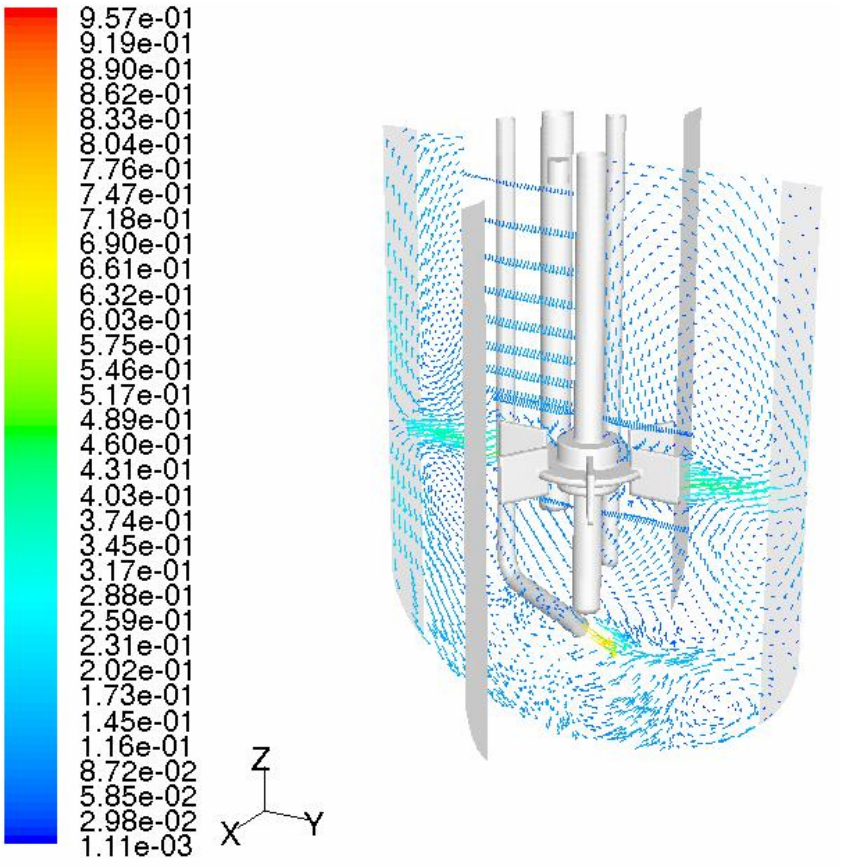

Figure 2 Velocity distributions for turbulent flow The volume of the tank is 1.4 liter, and the inlet (and outlet) flow rate is 40 mL/min, the mixing rate is 80 rpm.

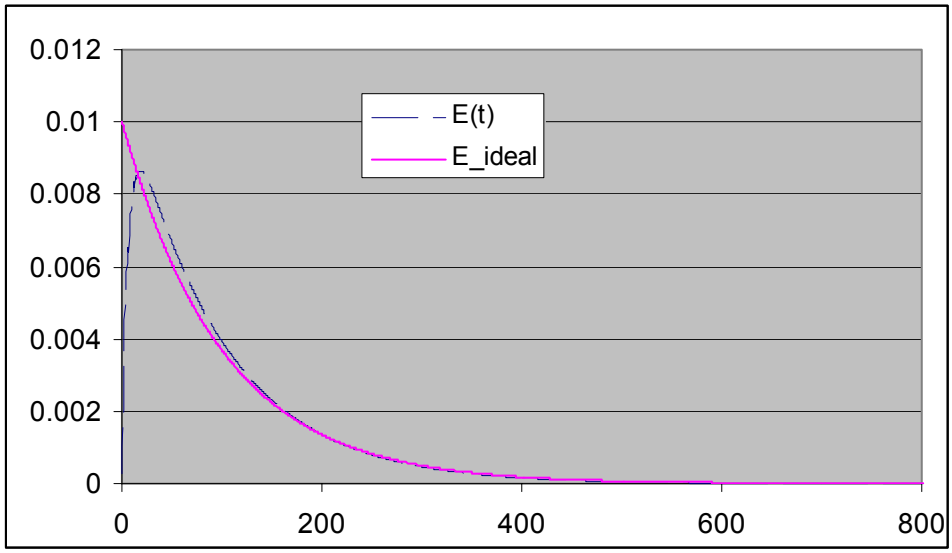

Figure 3 Comparison of Residence Time Distributions for Turbulent Flow Simulations with Ideal Well-Mixed Tank (-) with the Equation, $E(t)=1/\tau * \exp(-t/\tau)$, $\tau = V/Q$.

The mean and standard deviation of the residence time distribution was determined giving the following comparison in Table 2.

Table 2 Comparison of the Mean and Standard Deviation of the Residence Time Distributions for a 1.4 L tank with a feed flow rate of 40 mL/min and a mixing rate of 80 rpm.

	$t_{mean}/(V/Q)$	Error %	Std.Deviation/t_{mean}	Error %
CFD Turbulence Simulation	1.00199	0.2	0.94402	5.598
Perfect mixing	1	0	1	0

Ideal values for both the mean time, t_{mean}, divided by the ratio of tank volume, V, to volumetric flow rate, Q and the standard deviation divided by the mean time should be 1.0 if the mixing is ideal. The turbulent flow model approximates these values to within 0.2% error on the mean residence time and to 5.6% error in the standard deviation of the residence time distribution and was shown to be as accurate as the experiments themselves [Choi, B-S., et. al. (2004)]. The population balance simulations were performed with the same tank mixing rate since this mixing rate gives nearly ideal mixing conditions.

3. Numerical Case Studies

Numerical cases have been developed to test the QMOM CFD algorithm. First of all the velocity field was solved to a convergence of 10^{-5} for turbulent flow. Then a particulate multiphase calculation was initiated with the PBE solved by QMOM using 6 length-based moments 0 to 5 (or more precisely 3 lengths and 3 weights) with the velocity field fixed. The convergence criterion is lowered to 10^{-4} (or lower) for the multiphase PBE calculation with a relaxation parameter of 0.9 except when otherwise stated.

Case 1-Nucleation and Growth: The analytical solution to the PBE, equation [1], for nucleation and growth was obtained by setting the growth rate to a constant ($G(v)=G_0$), the aggregation kernel, $\beta(v,w)$, and the specific rate of breakage, $S(v)$, to zero. For this case the feed particle size distribution is set to zero, $n_{in}(v)=0$ and the boundary condition is

$$n(0) = n_o \qquad [13]$$

where n_o is the number density of particles with a zero size. The nucleation rate is given by the product of G_o and n_o. The analytical solution for this case is given by [Randolph, A. D. (1988)]

$$n(x) = n_o \exp(\frac{-x}{G_o \tau}) \qquad [14]$$

This analytical solution is converted to length-based moments for comparison with the simulation. The simulation was run with $G_{L\text{-}0}$=0.01 mm/s noting the above conversion in equation 12 and the nucleation rate was 1#/m^3/s. The mean residence time, τ, was 100 s for this simulation with no particles in the feed. The results of this comparison are given in Table 4 for a convergence criterion of 10^{-9}. Here we see that the simulation is in error by ~ 23% for the 5th length based moment.

Table 4 Moment comparison of PBE for QMOM simulations with analytical solution for nucleation and growth.

	Inlet	Outlet		
		Analytical	QMOM simulation	Error %
$_Lm_0$	0	100	100.88896	0.889
$_Lm_1$	0	100	96.458548	3.541
$_Lm_2$	0	200	183.72358	8.138
$_Lm_3$	0	600	522.45701	12.924
$_Lm_4$	0	2400	1970.7903	17.884
$_Lm_5$	0	12000	9257.3487	22.855

Figure 4 a & b shows $_Lm_0$ distribution inside tank. The $_Lm_0$ value indicates total number of particles per unit volume. We can see that $_Lm_0$ value at the inlet is very low and close to zero. That's because there is neither particles nor nuclei coming from the inlet. Then due to nucleation, there are particles created in the tank. In the upper part of the tank, the particle density is higher. We might expect that there is some segregation in a stirred tank but with segretation the higher particle density (and larger particle size, Figure 4c) should be found in the bottom of the tank or at the outside radius of the tank. The higher particle density in the upper part of the tank in Figures 4a & c is caused by a longer residence time in that circulation cell where more particles are nucleated when the residence time is longer. At the impeller level moving from top to bottom, there is an abrupt decrease in the total number of particles. In Figure 4b we see the $_Lm_0$ (particle density) profile at the impeller level. The total number of particles is less in the annular zone between the impeller and the feed tubes and thermowell because the material from the lower circulation cell is being transported upward in this zone. Behind the baffles and behind the feed tubes and thermo well, the total number of particles is higher because there are recirculation zones with longer residence times there. In Figure 4c the $_Lm_1$ moment profile, indicating the total

particle length, is shown to be of identical shape to the ${}_{L}m_0$ profile in Figure 4a. This is the case because both the nucleation rate and the growth rate are constants in this simulation so that the age distribution of the fluid can be observed with both increasing number of particles and increasing the size of the particles.

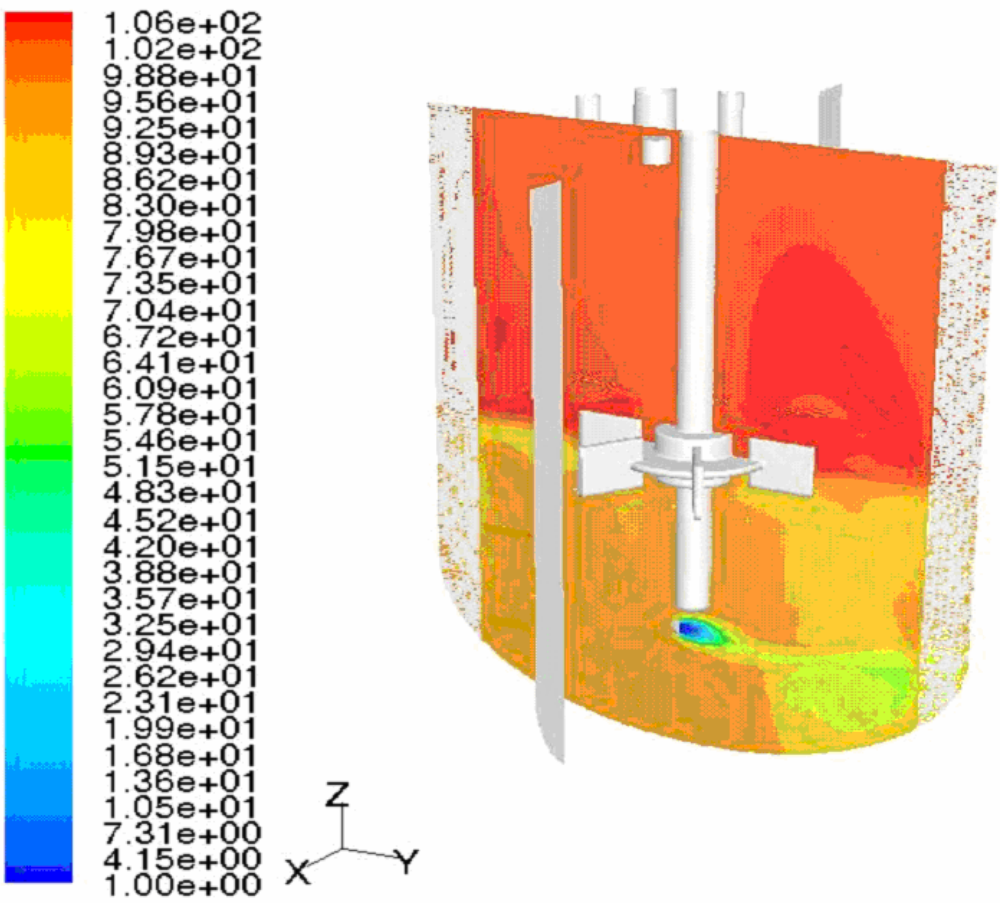

Figure 4a. Zeroth length based moment ${}_{L}m_0$ profile.

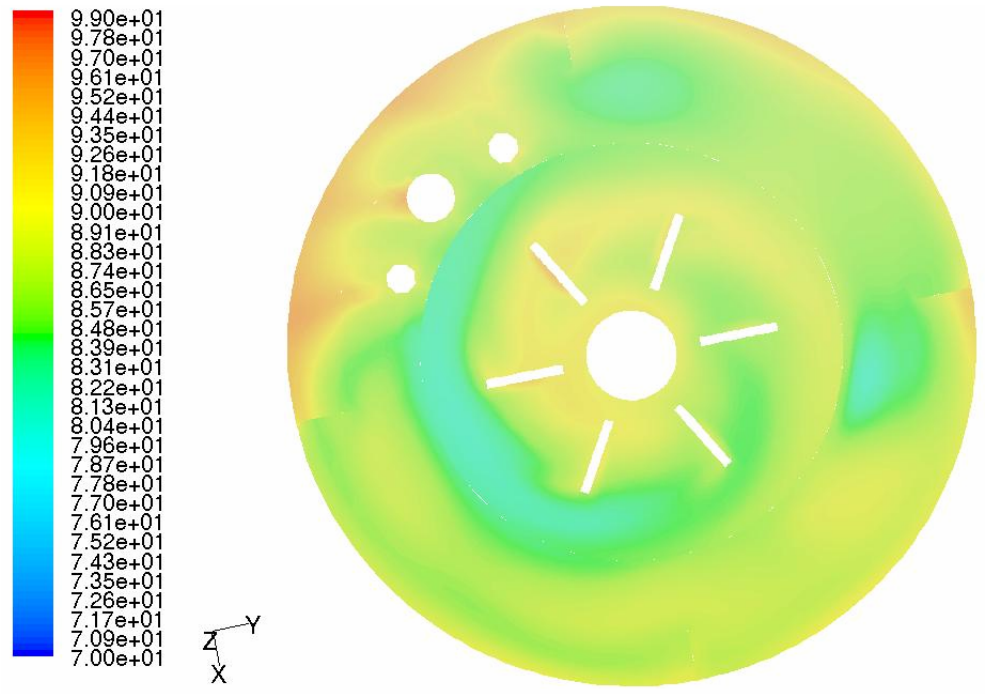

Figure 4b Zeroth length based moment ${}_{L}m_0$ moment profile, top view at the level of the impeller:

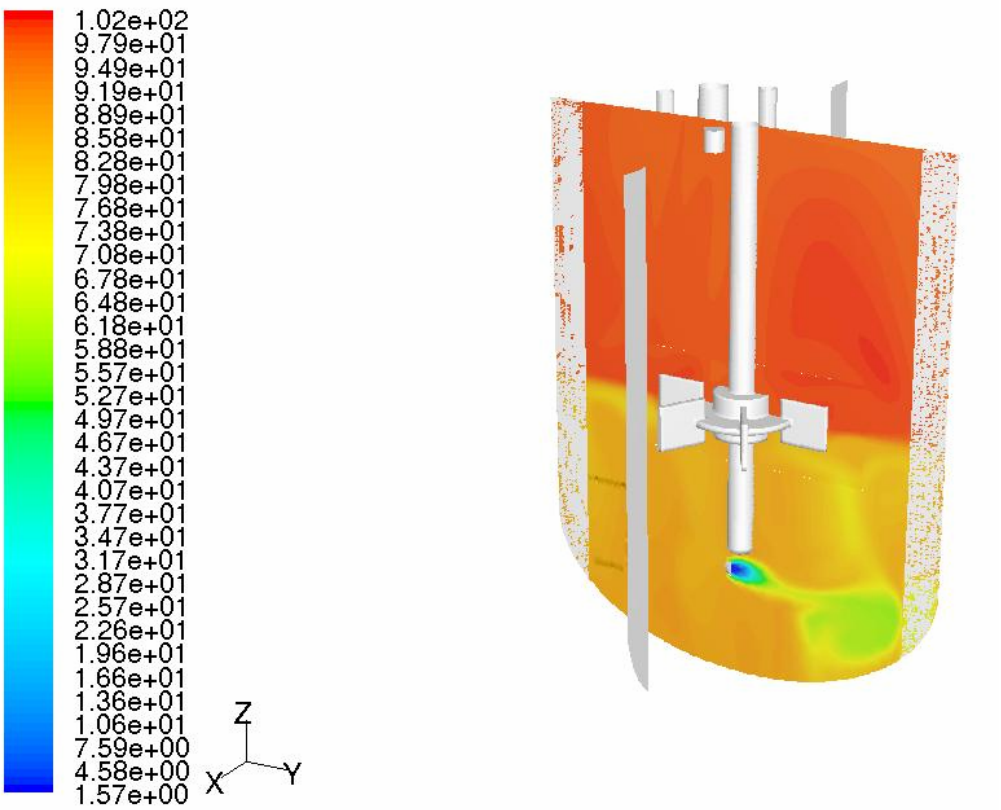

Figure 4c First length based moment ${}_{L}m_1$ profile.

Figure 4. Moment profiles in a 1.4 L stirred tank operating at mean residence time of 100 s and mixing rate of 80 rpm for Case-1 Nucleation and Growth. Figure 4a and 4b are ${}_{L}m_0$ moment (particle density) profiles. Figure 4c is the ${}_{L}m_1$ moment (total particle length) profile.

Case 2-Aggregation: The analytical solution to the PBE, equation [1], for aggregation alone was obtained by setting the growth rate to zero (G(v)=0), the aggregation kernel to a constant, $\beta(v,w)= \beta_o$, and the specific rate of breakage, S(v), to zero. For this case the feed particle size distribution is set to an exponential distribution given by:

$$n_{in}(v) = \frac{N_o}{v_o}\exp(\frac{-v}{v_o}) \qquad [2\text{-}1]$$

The analytical solution for this case is given by [Hounslow, M.J. (1990)]

$$n(v) = \frac{N_o}{v_o}\cdot\frac{I_o\left[\frac{-(\beta_o\cdot N_o\cdot\tau)\cdot v}{v_o\cdot\left[1+2\cdot(\beta_o\cdot N_o\cdot\tau)\right]}\right] + I_1\left[\frac{-(\beta_o\cdot N_o\cdot\tau)\cdot v}{v_o\cdot\left[1+2\cdot(\beta_o\cdot N_o\cdot\tau)\right]}\right]}{\sqrt{1+2\cdot(\beta_o\cdot N_o\cdot\tau)}\cdot\exp\left[\frac{(1+\beta_o\cdot N_o\cdot\tau)\cdot v}{\left[1+2\cdot(\beta_o\cdot N_o\cdot\tau)\right]v_o}\right]} \qquad [15]$$

where $I_o(z)$ and $I_1(z)$ are modified Bessel Functions of the first kind of zero and first orders. This analytical solution is converted to length-based moments for comparison with the QMOM simulation. Analytical expressions [Smit, D. J. (1993)] for the zeroth, first and second volume based moments are

$$\begin{aligned} {}_{v}m_0 &= \frac{-1+\sqrt{1+2\beta_o\, {}_{v}m_{0,in}\tau}}{\beta_o\tau} \\ {}_{v}m_1 &= {}_{v}m_{1,in} \\ {}_{v}m_2 &= {}_{v}m_{2,in} + \tau\ \beta_o\ {}_{v}m_1^2 \end{aligned} \qquad [16]$$

The QMOM simulation was run for the conditions of β_o=1 m^4/s, N_0=100 1/m^3, v_0=100 μm^3, and a mean residence time of 100 s with the relaxation factor set to 0.9. The simulation ran for 1,000 iterations to a convergence criterion of 10^{-6}. The results of this comparison are given in Table 5. Here we see that the simulation is accurate to ~6% and the 3rd length based moment, ${}_{L}m_3$, equivalent to the total particle volume, is accurately predicted to essentially not change in the tank with aggregation alone.

Table 5 Moment Comparison of PBE for QMOM Simulation with Analytical Solution for Aggregation Alone.

	Inlet	Outlet		
		Analytical	QMOM Simulation	Error %
$_Lm_0$	1	0.132	0.12418192	5.923
$_Lm_1$	1.108	0.225	0.22066035	1.929
$_Lm_2$	1.39	0.547	0.54765437	0.12
$_Lm_3$	1.91	1.91	1.9099633	0.001921
$_Lm_4$	2.821	9.073	9.0124754	0.667
$_Lm_5$	4.423	53.797	52.352038	2.686

Figure 5 shows the zeroth (a), first (b), third (c) length based moment profiles in the tank. In Figure 5a, the zeroth moment equivalent to the total number of particles is largest at the inlet. From the inlet the zeroth moment dissipates to an on average lower value in the lower circulation cell below the impeller. The zeroth moment is slightly smaller in the upper circulation cell above the impeller since the residence time is larger in the upper circulation cell and with longer time the particles aggregate more decreasing the particle number in the upper circulation cell. In Figure 5b, the first moment, $_Lm_1$, or total particle length profile for the tank. This profile is similar to that of the zeroth moment, $_Lm_0$, because the total length of particles gets smaller due to aggregation. In Figure 5c, the third moment, $_Lm_3$, or total volume of particles is every where nearly a constant as it should be for the aggregation process, see scale as well as figure.

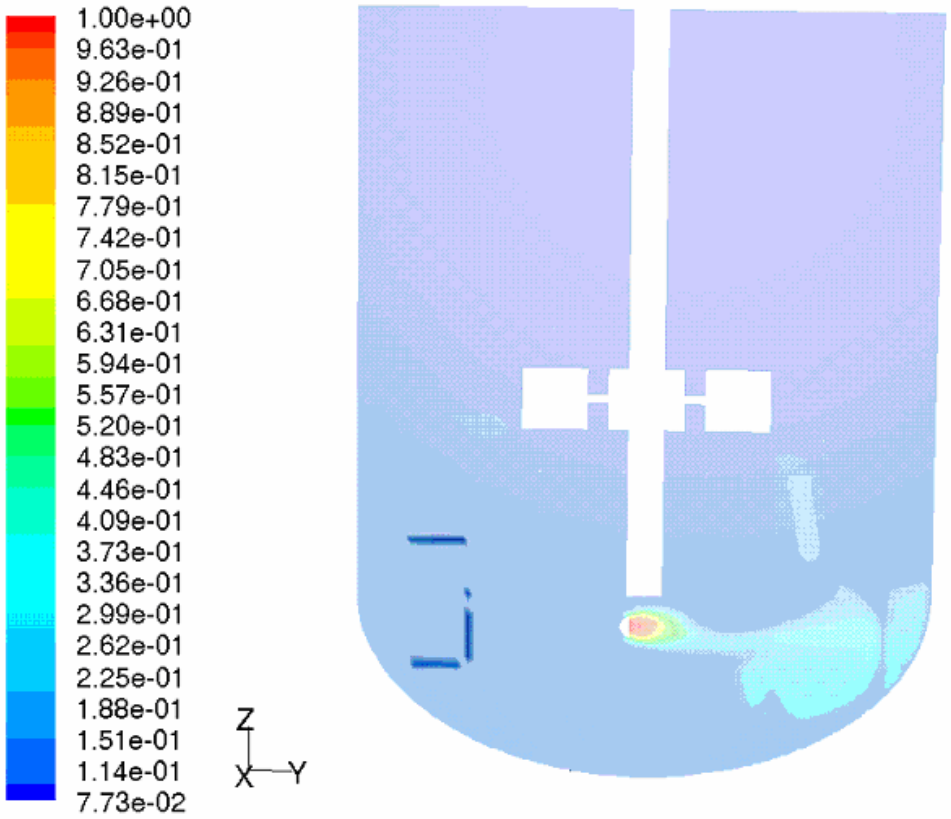

Figure 5a Zeroth length based moment $_{L}m_{0}$ profile for aggregation only case, front view

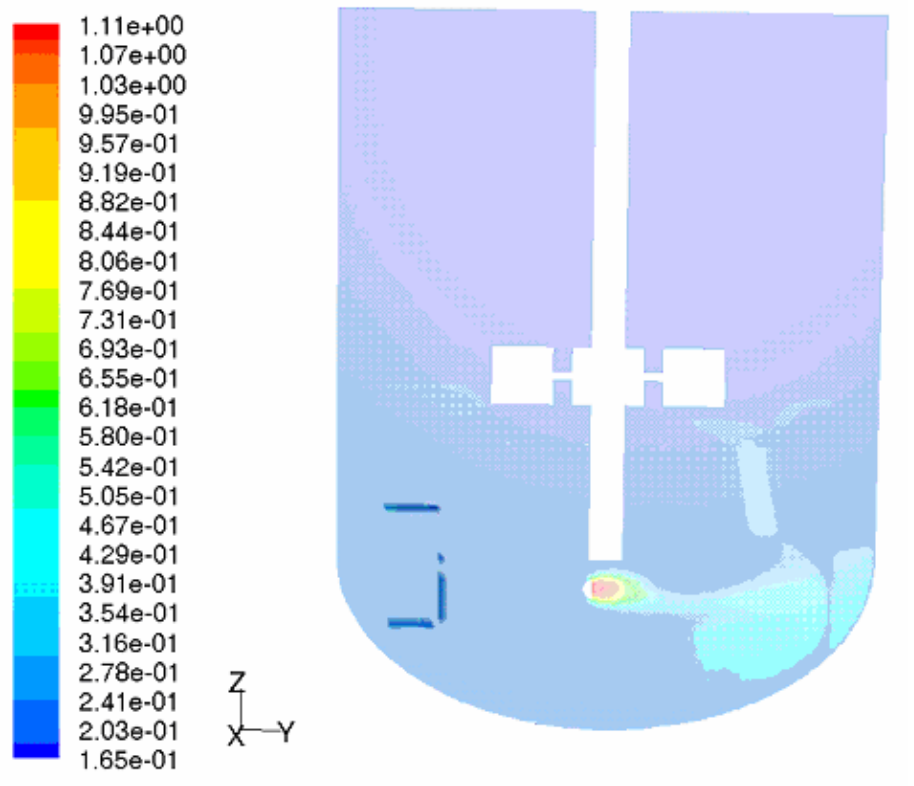

Figure 5b First length based moment $_{L}m_{1}$ profile for aggregation only case, front view

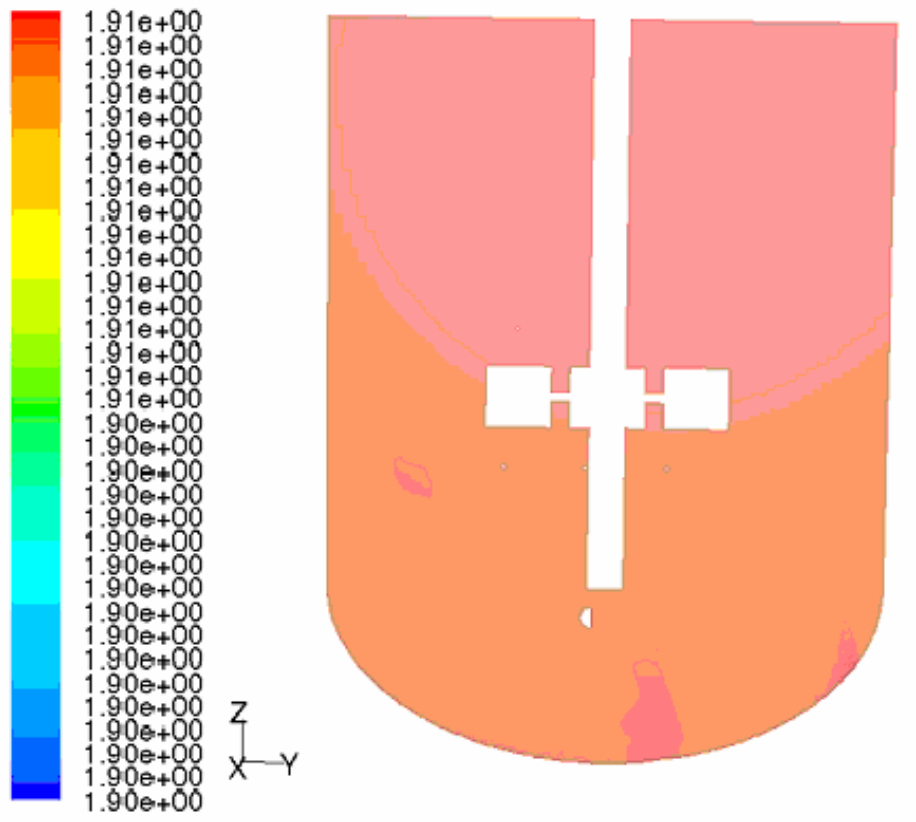

Figure 5c Third length based moment ${}_{L}m_3$ profile for aggregation only case, front view, different colors indicates numerical errors of 0.01%.

Figure 5. Moment profiles in a 1.4 L stirred tank operating at mean residence time of 100 s and mixing rate of 80 rpm for Case-2 Aggregation. Figure 5a is the ${}_{L}m_0$ moment (particle density) profile. Figure 5b is the ${}_{L}m_1$ moment (total particle length) profile. Figure 5c is the ${}_{L}m_3$ moment (volume of particles) profile, which is essentially a constant.

Case 3-Breakage: The analytical solution to the PBE, equation [1], for breakage alone was obtained by setting the growth rate to zero (G(v)=0), the aggregation kernel to zero, β(v,w)= 0, the specific rate of breakage to S(v)=v 1/s and the daughter distribution function is set to ρ(v,w)=2/w. For this case the feed particle size distribution is set to an exponential distribution.

The analytical solution for the case is given by [Nicmanis, M. (1998).]:

$$n(v) = \frac{N_o\left[(1+\tau v)^2 + 2\tau v_o\left(1+\tau\left(v_o+v\right)\right)\right]}{v_o(1+\tau v)\exp\left(\frac{v}{v_o}\right)} \qquad [17]$$

This analytical solution is converted to length-based moments for comparison with the QMOM simulation.

Analytical expressions of the zero[th] and first volume moments can be derived to give

$$
\begin{aligned}
{}_{v}m_{o} &= \tau\,{}_{v}m_{1} + {}_{v}m_{o,in} \\
{}_{v}m_{1} &= {}_{v}m_{1}
\end{aligned}
\qquad [18]
$$

which indicate that the volume of particles equivalent to the third length based moment is conserved. These moments are converted to length-based moments for direct comparison with the QMOM simulation.

The QMOM simulation was run with constants N_0 and v_0 were set to unity, the mean residence time, τ, of 100s. The simulation was run for 21,900 interations to get to a convergence criterion of 10^{-5}. Comparison of the simulation to the analytical solution is given in Table 6. The results for ${}_{L}m_3$ moment are accurately predicted indicating that mass is conserved. A plot of the ${}_{L}m_3$ moment profile showed a constant value at all locations just like Figure 6c. The errors for other moments are within 6.1%. Plots of the other moment profiles are similar to those for Case 2 - aggregation alone except that the upper circulation cell has slightly more particles, ${}_{L}m_0$, and larger particles, ${}_{L}m_1$, than the lower circulation cell.

Table 6 Moments Comparison of QMOM Simulation to the Analytical solution for Breakage only.

	Inlet	Outlet		
		Analytical	QMOM simulation	Error %
${}_{L}m_0$	1	101	94.746816	6.191
${}_{L}m_1$	1.108	21.758	20.595363	5.343
${}_{L}m_2$	1.39	5.807	5.608233	3.423
${}_{L}m_3$	1.91	1.91	1.9099698	1.581E-3
${}_{L}m_4$	2.821	0.789	0.79229203	0.417
${}_{L}m_5$	4.423	0.422	0.41217964	2.327

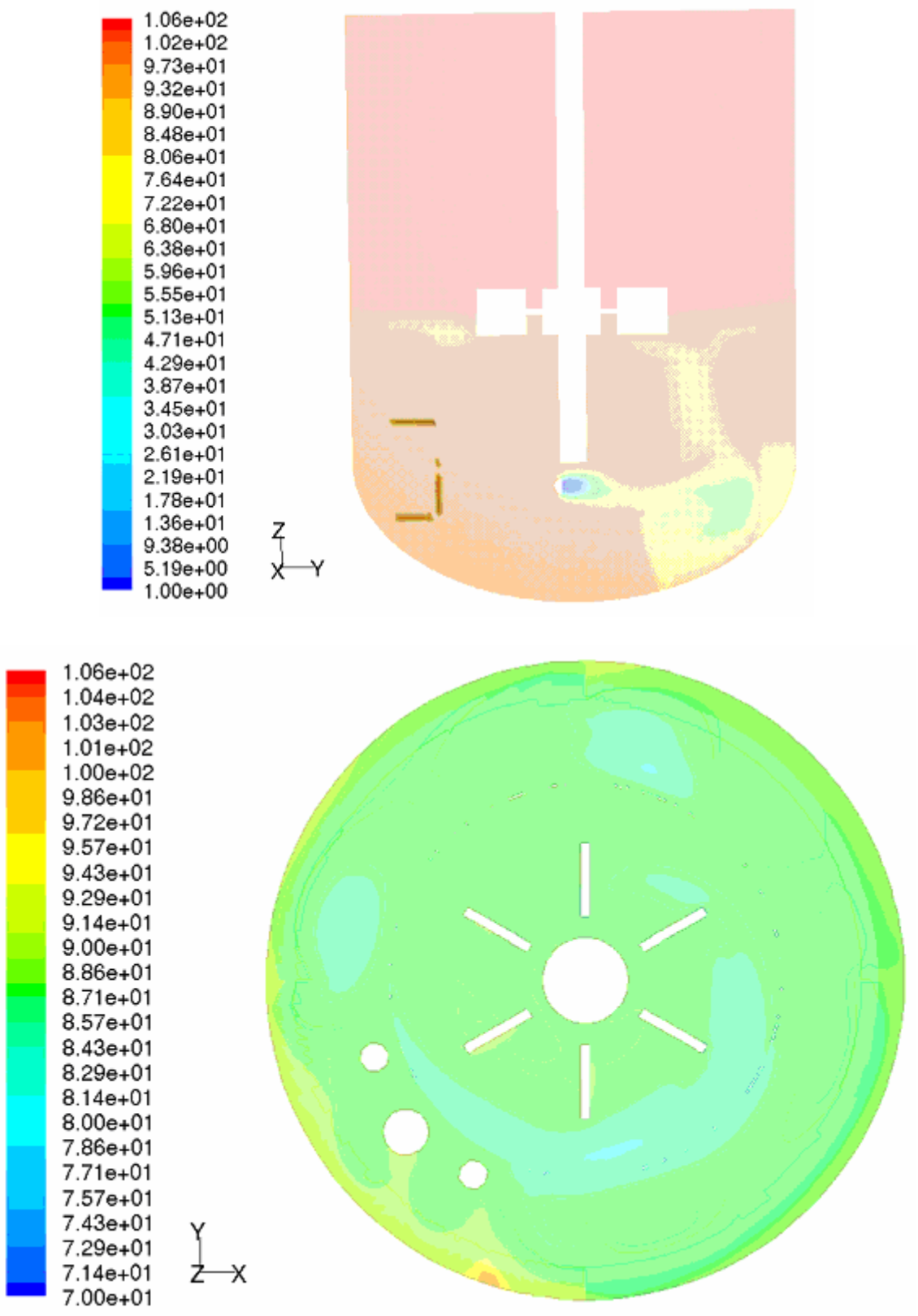

Figure 6a Front view and top view of $_{L}m_{0}$ contour for breakage case.

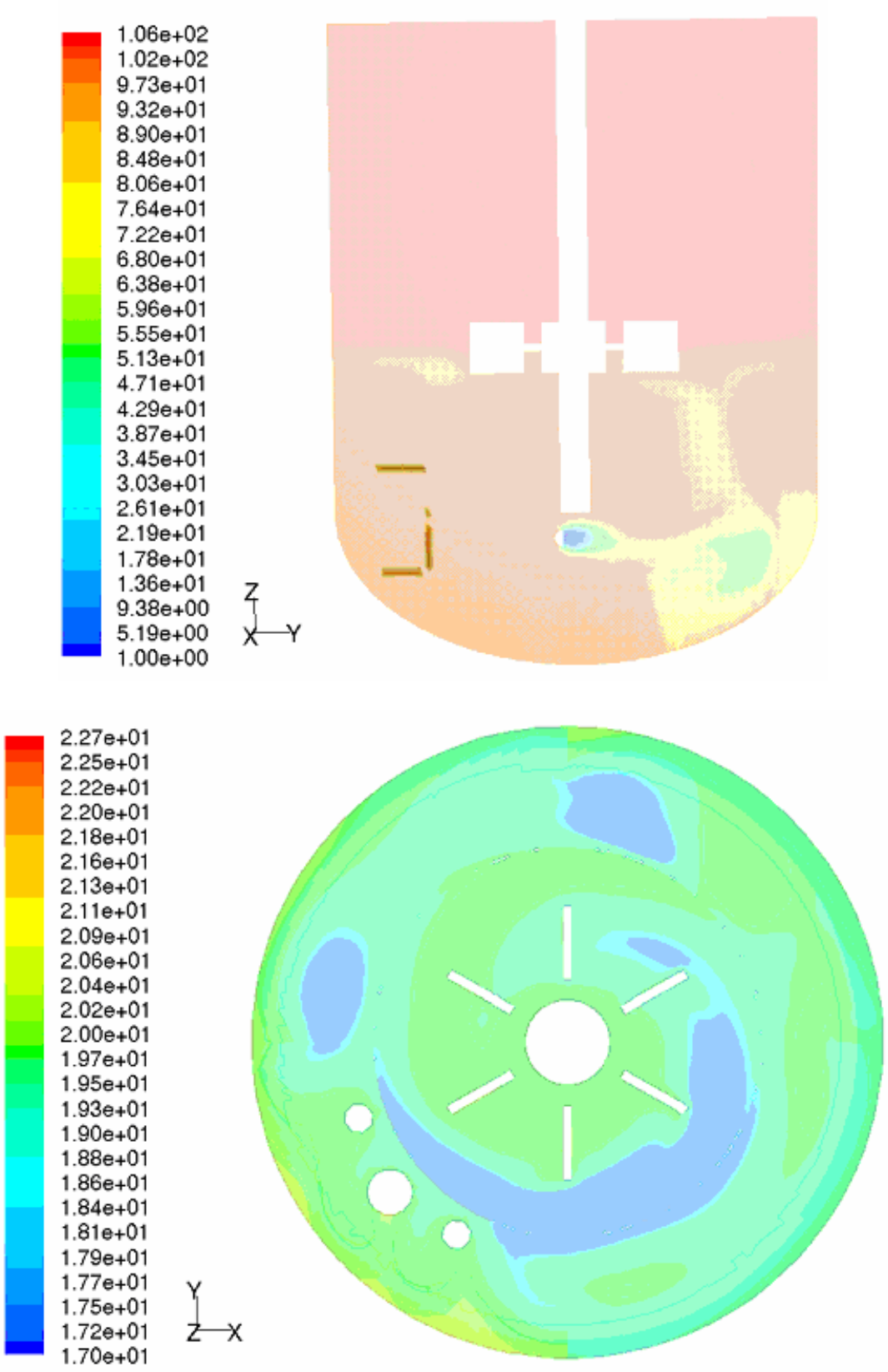

Figure 6b Front view and top view of $_{L}m_{1}$ contour for breakage case.

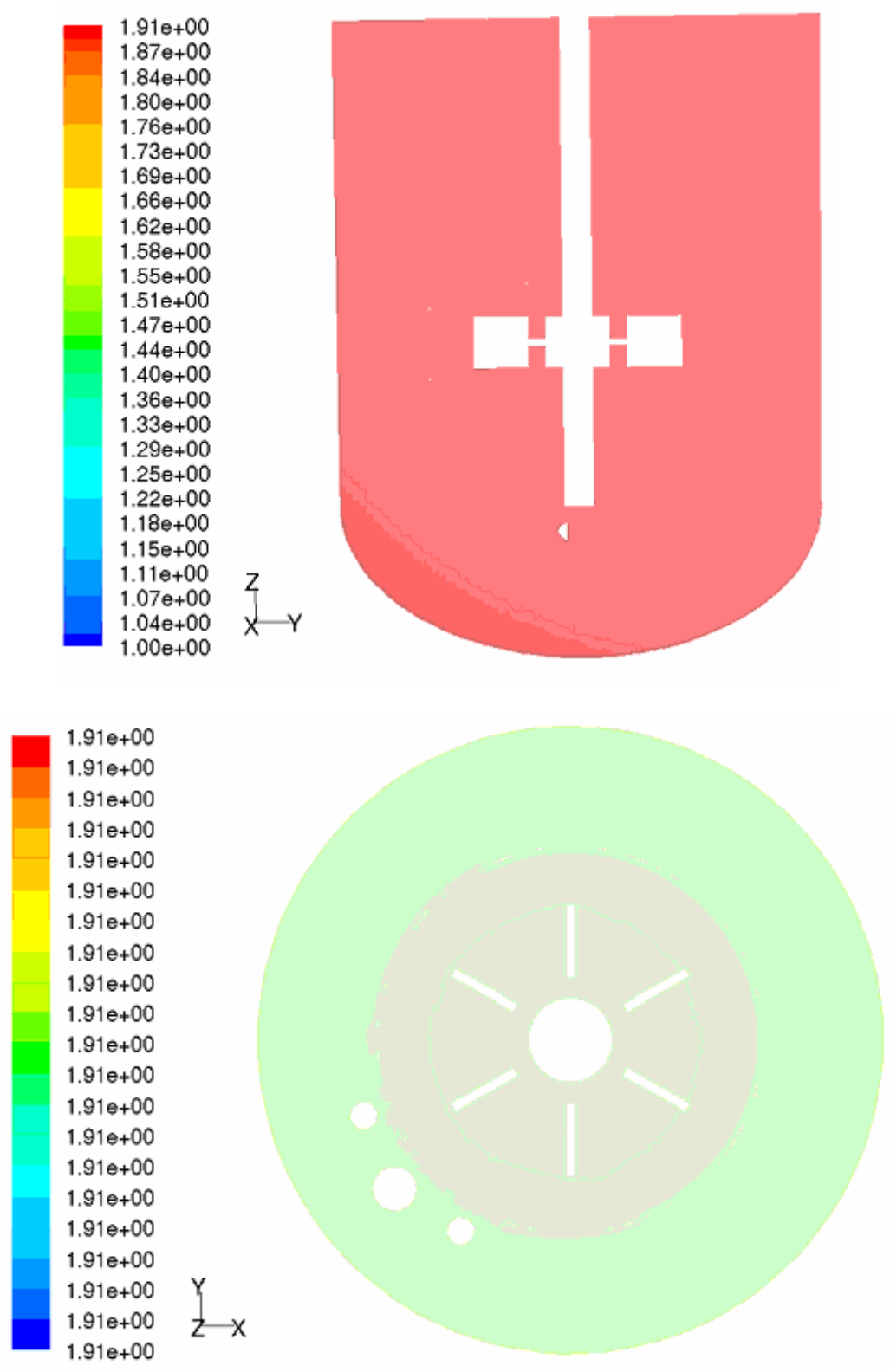

Figure 6c Front view and top view of $_{L}m_{3}$ contour for breakage case.

Figure 6. Moment profiles in a 1.4 L stirred tank operating at mean residence time of 100 s and mixing rate of 80 rpm for case-3 breakage. Figure 6a is the ${}_{L}m_0$ moment (particle density) profile. Figure 6b is the ${}_{L}m_1$ moment (total particle length) profile. Figure 6c is the ${}_{L}m_3$ moment (volume of particles) profile, which is essentially a constant.

Case 4-Nucleation, Growth and Aggregation Combined: The analytical solution to the PBE, equation [1], for nucleation, growth and aggregation combined was obtained by setting the growth rate to a constant ($G(v)=G_0$), the aggregation kernel to a constant, $\beta(v,w)= \beta_o$, and the specific rate of breakage, $S(v)$, to zero. For this case the feed particle size distribution is set to zero, $n_{in}(v)=0$ and the boundary condition was a constant, $n(0)=n_o$, where n_o is the number density of particles with zero size. The nucleation rate is given by the product of G_o and n_o. The analytical solution for this case is given by [Liao, P.F. (1976)].

$$n(v) = 2\cdot n_o \cdot \frac{\exp\left[-\sqrt{1+\frac{1}{2\cdot\beta_o\cdot n_o\cdot G_o\cdot\tau^2}}\cdot\left(\frac{v}{G_o}\cdot\sqrt{2\cdot\beta_o\cdot n_o\cdot G_o}\right)\right]}{\frac{v}{G_o}\cdot\sqrt{2\cdot\beta_o\cdot n_o\cdot G_o}}\cdot I_1\left(\frac{v}{G_o}\cdot\sqrt{2\cdot\beta_o\cdot n_o\cdot G_o}\right) \qquad [20]$$

where $I_1(z)$ is the modified Bessel Function of the first kind of first order. Analytical expressions of the zeroth, first and second volume moments can be derived to give

$$\begin{aligned} {}_{v}m_0 &= \frac{-1+\sqrt{1+2\beta_o n_o G_o \tau}}{\beta_o \tau} \\ {}_{v}m_1 &= \tau\ G_o\ {}_{v}m_0 \\ {}_{v}m_2 &= 2\tau G_o\ {}_{v}m_1 + \tau\ \beta_o\ {}_{v}m_1^2 \end{aligned} \qquad [21]$$

This analytical solution and the above moment equations are converted to length based moments for comparison with the QMOM simulation. The simulation was run with a volumetric growth rate, $G_{v\text{-}0}$, of 0.01 mm^3/s, which is equivalent to a length based growth rate, $G_{x\text{-}0}$, of $0.01/(kv*x^2)$ mm/s where x is the particle size. The aggregation kernel, β_o, was 0.1 m^4/s, the nucleation rate was 0.01 $1/m^3/s$ and the mean residence time, τ, was 100 s with no particles in the feed. The solution took 8000 iterations to reach a convergence criterion of 10^{-4} for the simulation. The results of the simulation compared to the analytical solution, equation [20], are given in Table 7. For the QMOM simulation, the largest error is 0.64% in the length moment, ${}_{L}m_1$.

Table 7 Moments comparison of QMOM turbulent simulation to the analytical solution to the PBE for nucleation, growth and aggregation

	Inlet	Outlet		
		Analytical	QMOM simulation	Error %
$_{L}m_0$	0	0.358	0.36013501	0.596
$_{L}m_1$	0	0.346	0.34603996	0.012
$_{L}m_2$	0	0.434	0.43654082	0.585
$_{L}m_3$	0	0.684	0.68825631	0.622
$_{L}m_4$	0	1.305	1.3131342	0.623
$_{L}m_5$	0	2.904	2.9222183	0.627

Figure 7 shows the moment profiles in the tank. In Figure 7a the $_{L}m_0$ moment profile corresponding to the total number of particles is shown. As the flow enters just below the impeller without particles, nucleation takes place and particles are produced increasing the number of particles as the flow moves away from the feed port. The mixing with other fluid in the tank dilutes and makes more uniform the particle number density. In the upper circulation cell above the impeller the number density of particle is slightly higher than in the lower circulation cell due to the longer residence time in the upper circulation cell. The balance of nucleation and aggregation in this case lowers the total number of particles compared with Case-1 Nucleation and Growth - compare Figure 7a with Figure 4a. In Figure 7b, the $_{L}m_1$ moment profile corresponding to the total length of particles is shown and in Figure 7c the $_{L}m_3$ moment profile corresponding to the total volume of particles is shown. These figures have the same trends as Figure 7a, for longer residence time the total particle length per unit volume and the total particle volume per unit volume are larger when the time that the flow stays in the zone increases.

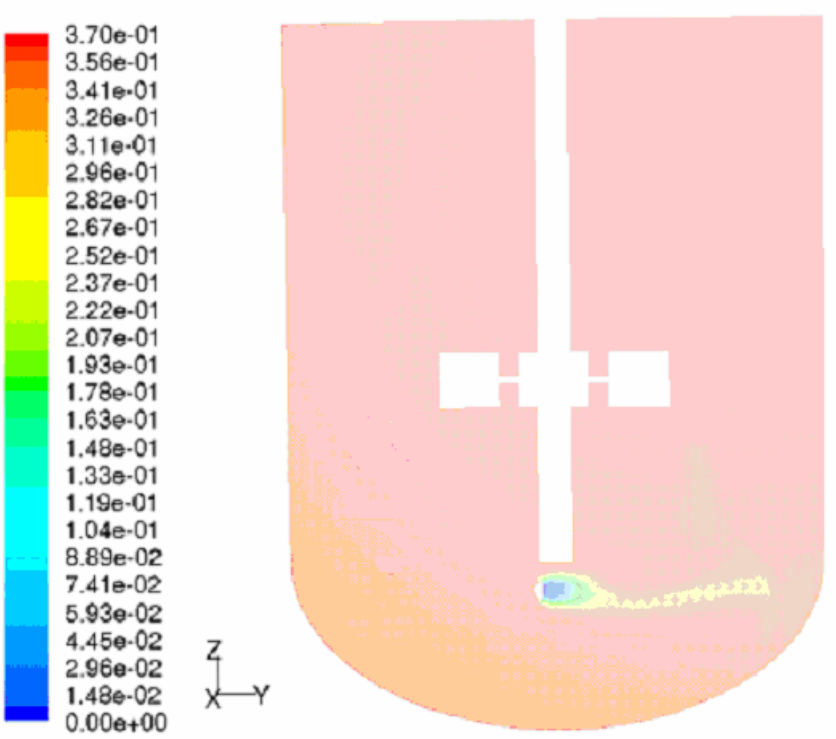

Figure 7a Zeroth length based moment ${}_{L}m_{0}$ profile

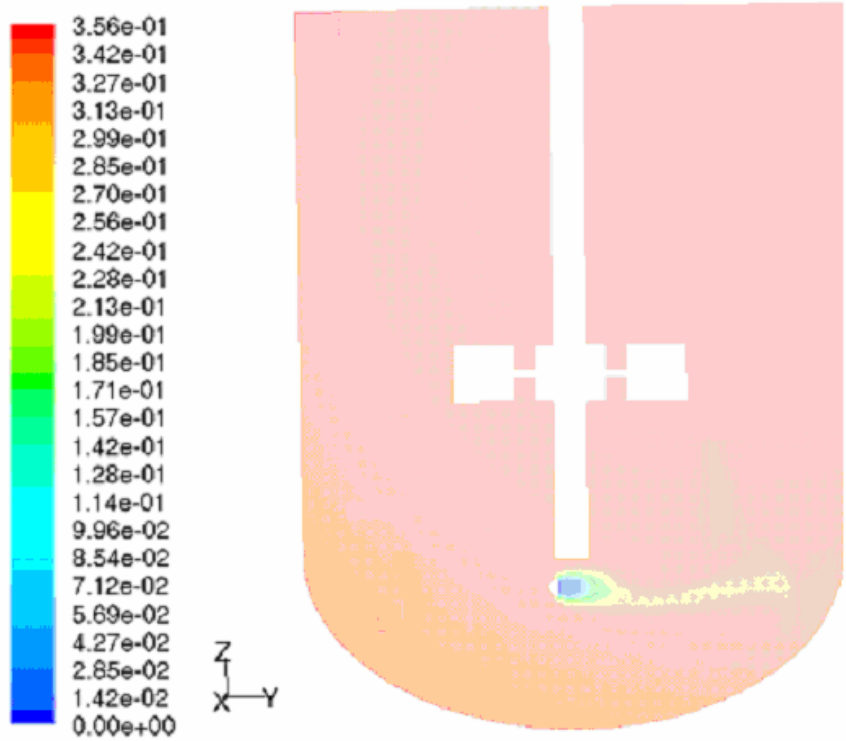

Figure 7b First length based moment ${}_{L}m_{1}$ profile

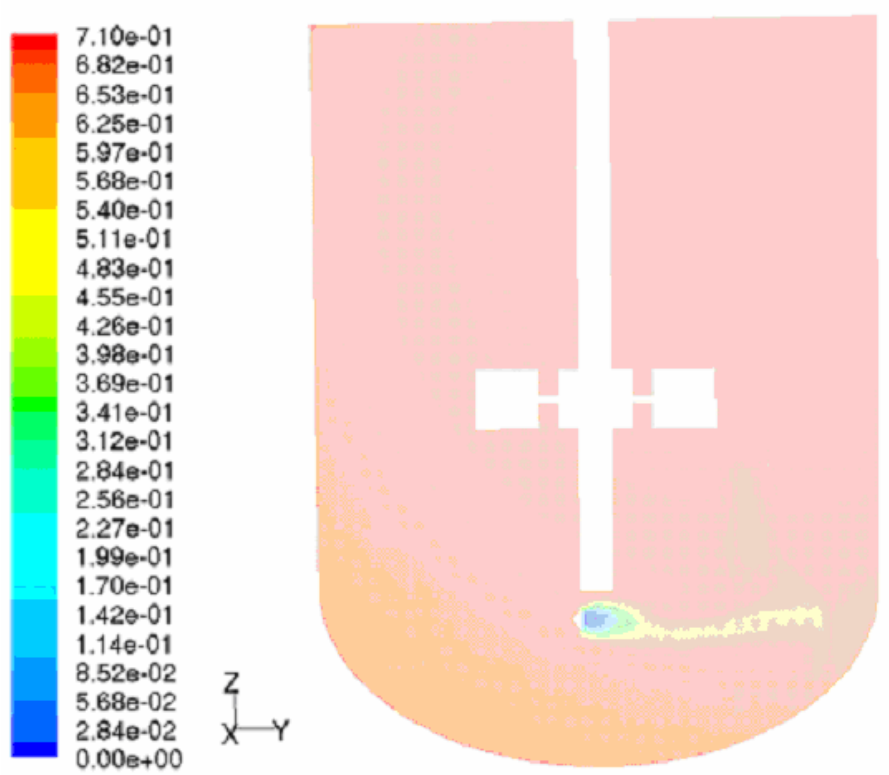

Figure 7c Third length based moment $_{L}m_3$ profile

Figure 7 Moment profiles in a 1.4 L stirred tank operating at mean residence time of 100 s and mixing rate of 80 rpm for case-4 combined nucleation, growth and aggregation case. Figure 7a is the $_{L}m_0$ moment (particle density) profile. Figure 7b is the $_{L}m_1$ moment (total particle length) profile. Figure 7c is the $_{L}m_3$ moment (total volume of particles) profile.

The results of these cases are in stark contrast to 2-D simulations of a well mixed tank that gave more accurate solutions for all of these cases [Wan, et. al., 2005]. The worst error with the 2-D solutions was with Case-3 Breakage where only a 0.4% error was observed in the first length based moment. The major difference in the residence time distribution between the 2-D and 3-D simulation was the deviation from ideality shown in Figure 3. In the 2-D case the ideal residence time was more accurately predicted. An additional difference was in the non-uniformity of the moment profiles. With the 2-D model the profiles were very uniform while for the 3-D model we have non uniform moment profiles especially at and below the impeller. As a result, we can attribute these errors in the simulations not to numerical problems with QMOM's numerical methods but to the non ideal mixing that this stirred tank has even when it is operated nearly ideally.

4. Conclusions

A 3-D CFD model of a 1.4 L well-mixed stirred tank with baffles, Rushton impeller and other internals was developed. Using a multiphase turbulence model a nearly ideal flow residence time distribution was validated. Using a two-phase model with a QMOM model of the PBE for the second, solid phase turbulent simulations were performed for cases with nucleation and growth, aggregation, breakage and nucleation, growth and aggregation combined. The simulations were compared with analytical solutions for a well mixed tank for those cases. The simulations were not particularly accurate with errors ranging from 0.6% to 22% depending upon the case. Errors from 5% to 20% were observed with most cases except the nucleation, growth and aggregation combined case where 0.6% error was observed. In this case the errors for aggregation and for nucleation and growth appear to cancel one another. These errors are not attributed to errors in QMOM or its implementation in the CFD code but to non ideal mixing in the tank.

Literature Cited:

Choi, B-S., Wan, B., Philyaw, S., Dhanasekharan, K. & Ring, T. A. (2004). “Residence Time Distributions in a Stirred Tank: Comparison of CFD Predictions with Experiment”, Ind. Eng. Chem. Res., 43(20) pp 6548 – 6556,

Hounslow, M. J. (1990). “A Discrete Population Balance for Continuous Systems at Steady State,” AIChE J., 36(1), 106.

Hulburt, H. M. & Katz, S. (1964) Some Problems in Particle Technology – Statistical Mechanical Formulation, Chem. Eng. Sci., 19, 555.

Liao, P. F. and Hulburt, H.M. (1976). “Agglomeration Processes in Suspension Crystallization,” AICHE Meeting, Chicago, December.

Marchisio, D.L., Virgil, R.D. and Fox, R.O. (2003). Quadrature Method of Moments for Aggregation-Breakage Processes, J. Colloid and Interface Sci., 258, 322-334.

McGraw, R. (1997), Description of Aerosol Dynamics by Quadrature Method of Moments, Aerosol Science and Technology, 27: 255-265.

Nicmanis, M. and Hounslow, M.J. (1998). “Finite-element Methods for Steady-State Population Balance Equations,” AIChE J., 44(10),2258-72.

Prasher, C.L. (1987), Crushing and Grinding Process Handbook, New York: Wiley

Randolph, A. D. & Larson, M. A. (1988) Theory of Particulate Processes, 2nd edition; New York: Academic Press

Smit, D. J., M. J. Hounslow, and W. R Paterson (1993). “Aggregation and Gelation 1: Analytical Solutions for CST and Batch Operation”, Chem. Eng. Sci, 49(7), 1025

Wan, B., Ring, T.A., Dhanasekharan, K.M. and Sanyal, J. (2005). “Comparison of Analytical Solutoins for CMSMPR Crystallizer with QMOM Population Balance Modeling in Fluent” China Particuology 3(4), 213-218